Ind. J. Pharm. Edu. Res., 2026; 60(2s):s507-s521.
https://www.ijper.org

Original Article

Molecular Dynamics Characterization of the NCA-II Binding Site in Insect $GABA_A$ Receptors and Its Application to Ligand Screening

Maria Salomé Gastaldi[1,2], Mariela Eugenia Sánchez-Borzone[1,2], Pran Kishore Deb[3], Supratik Kar[4], Katharigatta Narayanaswamy Venugopala[5,6,*], Daniel Asmed García[1,2,*], Virginia Miguel[1,2,*]

[1]Departamento de Química, Cátedra de Química Biológica, Facultad de Ciencias Exactas, Físicas y Naturales, Universidad Nacional de Córdoba, Córdoba, ARGENTINA.
[2]Instituto de Investigaciones Biológicas y Tecnológicas (IIByT), CONICET-Universidad Nacional de Córdoba, Córdoba, ARGENTINA.
[3]Department of Pharmaceutical Sciences and Technology, Birla Institute of Technology (BIT), Mesra, Ranchi, Jharkhand, INDIA.
[4]Department of Chemistry, Chemometrics and Molecular Modeling Laboratory, Kean University, 1000 Morris Avenue, Union, NJ, USA.
[5]Department of Pharmaceutical Sciences, College of Clinical Pharmacy, King Faisal University, Al-Ahsa, SAUDI ARABIA.
[6]Department of Biotechnology and Food Science, Faculty of Applied Sciences, Durban University of Technology, Durban, SOUTH AFRICA.

ABSTRACT

Objectives: The rapid evolution of insecticide resistance emphasizes the necessity for developing innovative approaches to discover novel insecticides that are highly selective and effective. The second generation of GABAergic Noncompetitive Antagonists (NCA-II), such as isoxazolines, constitutes a recent alternative in the design of new insecticides since they present high potency and selectivity. We aimed to contribute to the development of computational protocols that accelerate the search for new GABAergic insecticides, thereby reducing the costs and time required for their development. **Materials and Methods:** We performed Molecular Dynamics Simulations of canonical isoxazolines bound to *Aedes aegypti* $GABA_AR$, to characterize these insecticides interactions at the NCA-II binding site. Following this characterization, we used a protocol for an *in silico* screening of new compounds that act upon the NCA-II site, combining MDS with ligand and structure-based Virtual Screening. **Results:** MDS allowed us to identify the main energetic contributions to the interaction between isoxazolines and the receptor, including Van der Waals and hydrogen bonds with residues GLN219, THR257, and ASN264, among others. Additionally, we found that solvation at the binding site reduces this specific interaction. The screening protocol applied enabled us to identify a family of quinazolines with reported insecticidal activity that shares the key interactions previously described. These quinazolines have no reported protein target, and we hypothesize that the insect NCA-II binding site could be a potential target for this family. **Conclusion:** We believe that this approach offers a valuable strategy for accelerating the search and development of new potential GABAergic insecticides.

Keywords: *Aedes aegypti*, $GABA_A$ Receptor, Molecular Dynamics Simulations, Selective Insecticides, Virtual Screening, Molecular Docking.

Correspondence:
Dr. Katharigatta Narayanaswamy Venugopala
Department of Pharmaceutical Sciences, College of Clinical Pharmacy, King Faisal University, Al-Ahsa 31982, SAUDI ARABIA.
Email: kvenugopala@kfu.edu.sa
ORCID: 0000-0003-0680-1549

Dr. Daniel Asmed García
[1]Departamento de Química, Cátedra de Química Biológica, Facultad de Ciencias Exactas, Físicas y Naturales, Universidad Nacional de Córdoba, Córdoba, ARGENTINA.
[2]Instituto de Investigaciones Biológicas y Tecnológicas (IIByT), CONICET-Universidad Nacional de Córdoba, Córdoba, ARGENTINA.
Email: dagarcia@unc.edu.ar
ORCID: 0000-0001-5282-2557

Dr. Virginia Miguel
[1]Departamento de Química, Cátedra de Química Biológica, Facultad de Ciencias Exactas, Físicas y Naturales, Universidad Nacional de Córdoba, Córdoba, ARGENTINA.
[2]Instituto de Investigaciones Biológicas y Tecnológicas (IIByT), CONICET-Universidad Nacional de Córdoba, Córdoba, ARGENTINA.
Email: virgimiguel@unc.edu.ar
ORCID: 0000-0002-5651-6386

Received: 12-09-2025;
Revised: 29-10-2025;
Accepted: 08-12-2025.

DOI: 10.5530/ijper.20264008

INTRODUCTION

The γ-Aminobutyric Acid (GABA) is considered as the major inhibitory neurotransmitter in the nervous system of vertebrates and invertebrates. The family of isoxazoline ectoparasiticide/insecticides acts as a Noncompetitive Antagonist (NCA) or blocker of the $GABA_A$ Receptor ($GABA_A$R).[1] The scaffold isoxazoline has become one of the most recent alternatives in the design of new insecticides,[2] because of its high selective toxicity for insects versus mammals.[3] Isoxazolines present a unique structure, potency, and selectivity for insects compared with other GABAergic insecticides. This makes isoxazolines, which are the second generation of NCAs (NCA-II), preferred over first generation NCAs (NCA-I) such as fipronil, for which use has been restricted because of its high toxicity to fish and honeybees.[4,5] Afoxolaner was the first isoxazoline compound commercialized, followed by fluralaner, sarolaner, and the most recent lotilaner (Figure 1A).[6]

$GABA_A$Rs are pentameric proteins, and in humans, they are formed as combinations of homologous subunits encoded from a pool of 19 different genes.[7] Insect $GABA_A$Rs are known as Resistance to Dieldrin (RDL) receptors, because they are represented by a unique RDL subunit that forms functional homo-pentameric receptors with some pharmacological differences from most native mammalian $GABA_A$Rs.[8] Each RDL monomer has four Transmembrane Regions (TM1-TM4), with TM2 providing most of the residues that face the light of the chloride channel (Figure 1B).[9]

Isoxazolines are NCAs with a different high-affinity binding site on the RDL receptor than those of compounds such as NCA-IA, NCA-IB, and Avermectins 10. This NCA-II site differs enough between insects and mammals to confer selective toxicity.[10] It has been reported that isoxazolines bind to the Transmembrane Subunit Interface (TSI), which is facing the lipid phase. This binding site is formed by the TM1 and TM3 of two adjacent subunits, also involving TM2 residues.[11,12] Mutational and *in silico* assays have indicated that GLN271, ILE274, and LEU278 in TM1 are associated with the high sensitivity of *Musca domestica* RDL receptors to Fluralaner (Figure 1C).[11] Nevertheless, the site of action and the binding/inhibition mechanisms of these insecticides remain to be fully described.

Because of the emergence of resistance in insects to NCA-I and NCA-II insecticides, there is a constant need to develop novel ones that are highly selective and effective against pests. We have previously optimized a Structure-Based (SB) Virtual Screening (VS) process for the search of potential antagonists binding to the RDL NCA-IA site,[13] which is located inside the transmembrane pore, and where insecticide fipronil binds to exert its action. VS consists of computational analysis of large databases of chemical compounds, filtering the chemical space of available compounds, and finding a smaller subset of compounds that can potentially bind with high affinity for a protein site of interest, speeding up the rational drug design.[14] There are several VS techniques based on the properties of the ligands, such as pharmacophore-based methods and QSAR (quantitative structure-activity relationship) analysis.[15] On the other hand, Structure-Based VS (SBVS) makes use of the 3D structure of the target protein and docking for the estimation of the binding affinities of chemical compounds already studied.[16] To assess the performance of a SBVS, a "Retrospective" VS (RVS) must be carried out.[17] This requires that there is a significant number of chemical compounds that have been experimentally demonstrated as active ligands, and verification that the SBVS is capable of discriminating these active ligands from others that are inactive (decoys). Because of the incipient development of the isoxazoline family, large amounts of experimental data are not available to perform a proper retrospective SBVS. Therefore, we applied a hybrid protocol with Ligand-Based VS (LBVS) and SBVS, which strengthened the confidence of our results. A similar approach was recently used for the characterization of desmethylbroflanilide.[2] Also, Structure-Activity Relationship (SAR) investigations have been previously used for the design of novel isoxazoline benzoxaborole small molecules.[13]

In our study, we set a protocol for an *in silico* screening of new insecticides that act upon the isoxazoline binding site. In the process of developing such a protocol, we were able to better characterize the binding and modes of action of isoxazolines on RDL receptors. A three-Dimensional (3D) structure of *Aedes aegypti* RDL Receptor (*Aa*RDL) was constructed using the Glutamate-Gated Chloride Channel (GLUCl) in an open conformational state as a template (pdb:3RHW).[13] This model was used for docking and Molecular Dynamics Simulations (MDS) of canonical isoxazolines to characterize the binding mode of this family. A pharmacophore model was then generated based on the structural features of 7 isoxazolines with experimental K_d obtained from the bibliography,[2,18] which was used for filtering the ZINC database (https://zinc.docking.org/) to perform a docking-based VS. The applied screening protocol allowed us to identify another family of compounds, the quinazolines, with insecticidal and larvicidal activity already reported, which could recognize the NCA-II binding site of the RDL receptor, and for which no protein target had been previously described. MDS was also applied to characterize the binding site and the binding mechanism of these compounds, proposing RDL receptors as the target protein of insecticide quinazolines.

MATERIALS AND METHODS

In silico model selection for the receptor channel

Since no crystallographic structure is available for the RDL homopentamer, our group developed 10 different 3D models of *A. aegypti1*.[3] These were obtained by homology modeling, using the MODELLER program[19] from the amino acid sequence of the RDL

subunit of the receptor and the crystal structures of 10 different homo-pentamers belonging to the pLGIC superfamily, which were used as templates. The models were obtained and validated before the AlphaFold (https://alphafold.com/) appearance, and were kept as an option instead of the development of a new AlphaFold model, because we have previously validated these models for the optimization of protocols for the virtual screening of NCA-I insecticides.[13] These structures were obtained from the Protein Data Bank (https://www.rcsb.org/), and they correspond to different conformational states of the channel: open, closed, and desensitized (Table S1). The sequence was obtained from UniProtKB (https://www.uniprot.org/) (Code: Q16896) (Figure S1). The amino acid sequences of the templates have at least 30% sequence similarity with respect to the target sequence. Given the lack of suitable templates to model the sequence of the cytoplasmic loop of the intracellular domain of the RDL subunit, it was eliminated from the models obtained.[5] The performance of all possible TSIs of each model was evaluated by Molecular Docking assays, using AutodockVina[20] with default parameters (Figure S2). The model whose TSI best replicated both the spatial orientation of the fluralaner molecule at the receptor blocking site, reported by Sheng *et al.*, 2019[12] and Yamato *et al.*, 2020,[11] using molecular docking assays, as well as the interaction reported by Yamato et al., 2020,[11] through pharmacological assays, was selected.

Prospective Virtual Screening workflow

A prospective LBVS was performed following the workflow described in Figure 4A.[21] A set of 19 isoxazolines, with insecticidal activity reported in the literature,[2,18] was used to generate ligand-based pharmacophore models and subsequently validate a selected model using the LigandScout 4.4 program.[22] Seven (07) active ligands (*Training-set ligands*) were used for the generation of a pharmacophore model (Table S2). This set of ligands was selected based on the structural variability that exists between the molecules and the highest activity values reported for each one. The best pharmacophore model generated was validated by measuring its ability to discriminate between active ligands from decoys, using 12 active ligands (*Test-set ligands*) and 650 decoys, generated by the DUD-E tool[23] from these active ligands (Table S2).

Five pharmacophoric features (four hydrophobic type interactions and the presence of an aromatic ring, which establishes π-π and cation-π interactions) of the selected best model were used as a search element or query in the online interface ZINCPharmer[24] for the recovery of potential molecules of the ZINC database (containing approx. 20 million compounds available for purchase) (https://zinc.docking.org/). The search-retrieved compounds were used to carry out Molecular Docking tests, using the AutodockVina program[20] in the fluralaner binding site of the *in silico* model of the *Aa*RDL (Figure 1 B-C). All these calculations were performed using the Mulatona Cluster of CCAD-Universidad Nacional de Córdoba (http://ccad.unc.edu.ar/).

Molecular Docking

Molecular Docking at the NCA-II site of *Aa*RDL was performed using isoxazolines and the compounds obtained from the VS. AutoDock Vina 1.1.2, with its default calculation parameters, was used.[20] Blind Docking assays were carried out with a box that covered the entire transmembrane area of the *Aa*RDL and the crystallographic structure of the most abundant combination of subunits in mammals, $GABA_AR$, that is, $\alpha1\beta2\gamma2$[25] PDB ID: 6X3U.[26] The AutoDock Vina 1.2.5 program[20] with an exhaustiveness setting of 16[27] was used to increase exhaustiveness.

Molecular Dynamics Simulations

The simulated systems consisted of a pre-equilibrated hydrated lipid bilayer (502 molecules of POPC -palmitoyl-oleoyl phosphatidylcholine-, image18,900 molecules of water) with a ligand-receptor complex embedded. The following complexes with *Aa*RDL were used: fluralaner, afoxolaner, lotilaner, and sarolaner, including the resulting compounds of VS. Each ligand-receptor complex was inserted into the pre-equilibrated bilayer using the InflateGRO method.[28] The atomistic MDS of each of these systems was carried out for 500 ns using GROMACS v.2018.6 with GPU acceleration.[29] The *AMBER99SB-IDLN FF*[30] was used for the receptor and All Atom *Slipids*[31] for the POPC molecules, as well as the TIP3P[32] model for the water molecules. The temperature and pressure were kept constant at 300 K and 1 bar, with a Nosé-Hoover thermostat[33,34] and a Parrinello-Rahman barostat,[35] respectively. To obtain a model structure of these canonical isoxazolines and the virtual screened compound, we perform quantum calculations for the optimization of the geometry using the Gaussian 09 program, and determine the RESP (Restrained Electrostatic Potential) charge distribution with Gaussian 03 with a level B3LYP/6-31+G*.[36] Finally, the AnteChamber module and the GAFF[37] force field were used to get each topology of the molecule for its use in MDS. ACPYPE (AnteChamber Python Parser)[38] interface was used to obtain the topologies in the format required for GROMACS. All MDS were carried out in the Serafín Cluster of CCAD-Universidad Nacional de Córdoba (http://ccad.unc.edu.ar/).

Binding free energy calculation

The Molecular Mechanics/Poisson–Boltzmann Surface Area (MMPBSA) method was used to estimate end-state binding free energy (ΔG_{bind}) for each simulated system after reaching equilibrium. The calculations were carried out by GMX_MMPBSA software,[39] which combines functions from GROMACS[29] and AmberTools[40] in *MMPBSA.py* script[41] using the computational resources of Eulogia Cluster of CCAD-Universidad Nacional de Córdoba (http://ccad.unc.edu.ar/). This algorithm allows the inclusion of an implicit membrane in the calculation, that is, it

considers that the ligand-protein complex is embedded into the hydrated lipid bilayer.

The free binding energy for a complex can be estimated as follows:

$$\Delta G_{bind} = G_{complex} - G_{receptor} - G_{ligand} \quad (1)$$

In turn, ΔG_{bind} can also be represented as:

$$\Delta G_{bind} = \Delta E_{MM} - \Delta G_{sol} - T\Delta S \quad (2)$$

Where, ΔE_{MM} corresponds to the molecular mechanical energy changes in the gas phase, ΔG_{sol} is the solvation energy, and $T\Delta S$ is the conformational entropic contribution. ΔE_{MM} includes: Internal Energies (ΔE_{int}), Electrostatic Energies (ΔEele), and Van der Waals Energies (ΔE_{vdW}).

$$\Delta E_{MM} = \Delta E_{int} - \Delta E_{ele} - \Delta E \ (3)$$

The solvation energy ΔG_{SOL} considers polar (ΔG_{POLAR}) and nonpolar ($\Delta G_{NONPOLAR}$) contributions. The first component is calculated using the Poisson-Boltzmann model, and the second component is generally assumed to be proportional to the total Solvent Accessible Surface Area (SASA) of the molecule.

$$\Delta G_{sol} = \Delta E_{polar} - \Delta G_{npolar} - T\Delta S \ (4)$$

RESULTS AND DISCUSSION

In silico model selection

First, we used Molecular Docking assays to characterize the binding of isoxazolines on *Aa*RDL (Figure 1). Since there is no available crystallographic structure of the RDL homopentamer, we have previously developed 15 different 3D models of the *Musca domestica* RDL homopentamer based on 15 pLGIC templates whose structures had been determined in different conformational states of the channel: open, closed, and desensitized.[13] Following the same approach, we have obtained and validated 10 homology models of the insect *Aa*RDL homopentamer, including all conformational states (Table S1). The model of RDL homopentamer that showed the best binding energy estimated by AutoDock Vina[27] and that was capable of replicating the binding pose of the fluralaner molecule reported in a previous work by Sheng *et al.*, 2019[12] and YYamato et al.,2020,[11] (Figure 1 B-C), was selected (Figure S3 A). The model based on the crystal structure of *C. elegans* GluCl (PDB: 3RHW),[14] which presents an open conformational state, was used as a template

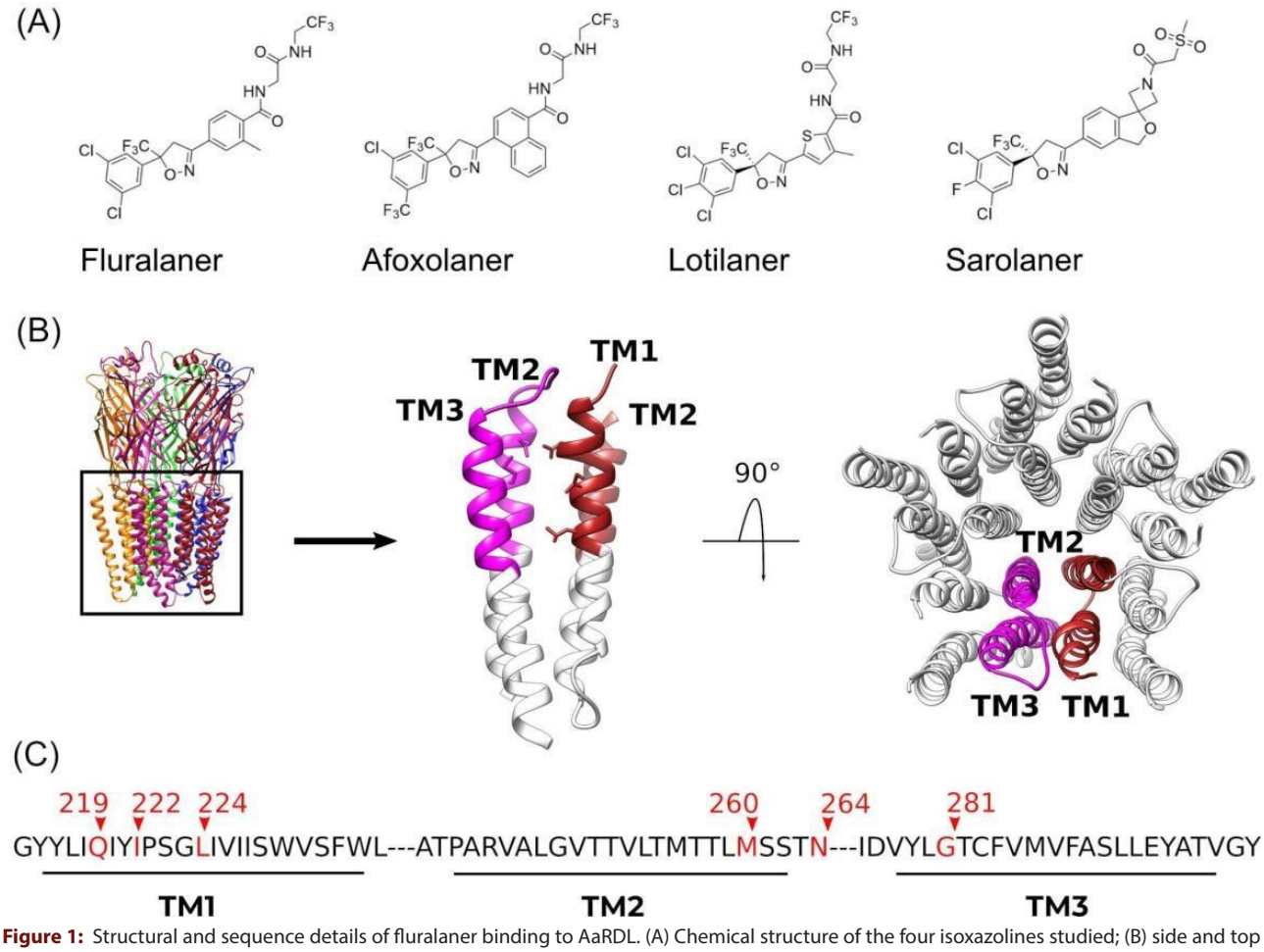

Figure 1: Structural and sequence details of fluralaner binding to AaRDL. (A) Chemical structure of the four isoxazolines studied; (B) side and top view of the fluralaner binding site inside the TM of the *Aa*RDL; (C) TSI amino acid sequences with the main residues involved in the fluralaner-receptor interaction.

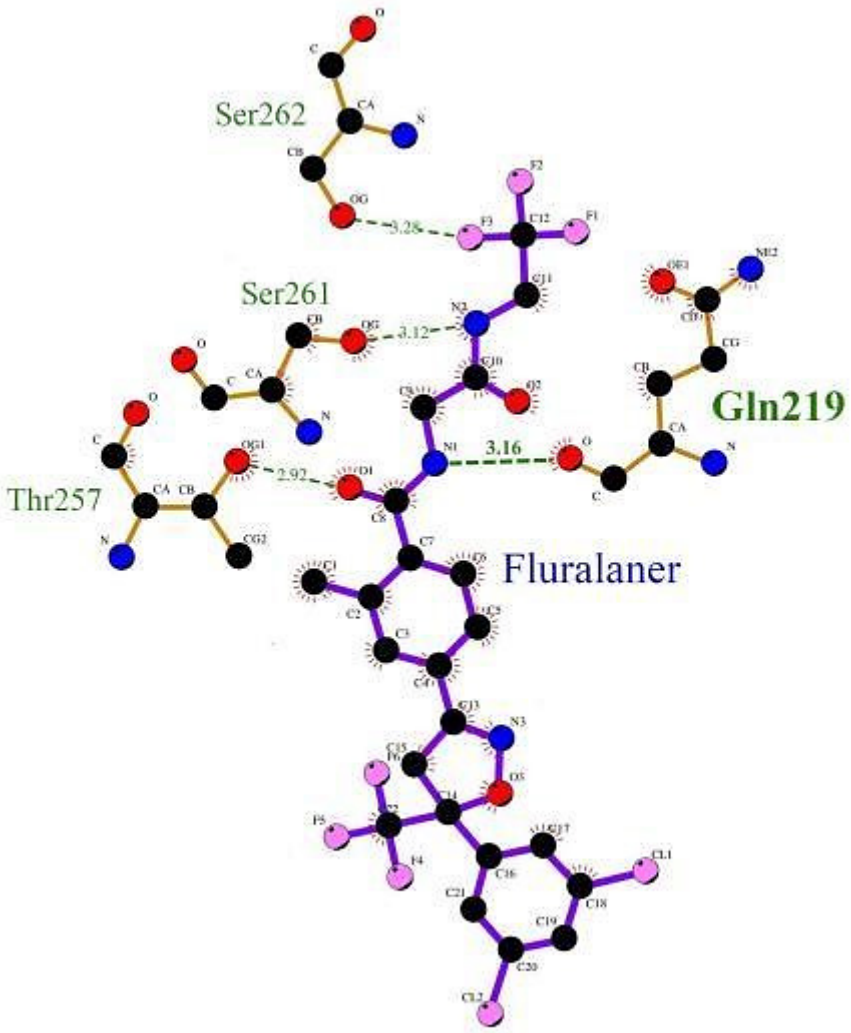

Figure 2: Representative LigPlot image of H-bond interaction (green dashed lines) between fluralaner and *Aa*RDL. Highlighting the hydrogen interaction between the amide group of fluralaner and the carbonyl oxygen of a GLN219 located in TM1. The results of docking of isoxazolines at the NCA-II binding site of *Aa*RDL showed that these molecules adopt a preferential binding pose similar to that predicted previously by Sheng *et al.*,[12] and Yamato *et al.*,[11] for fluralaner (Figure S3). Since there is no detailed information on the specific interactions at their binding site for the compounds afoxolaner, lotilaner, and sarolaner, we used fluralaner as a reference. The *Aa*RDL-isoxazolines complexes obtained by docking were used as starting structures of MDS (See next section).

for subsequent *in silico* assays. Docking assays using this model as a target replicated the pose of fluralaner bound between TM1 of a subunit and TM3 of the contiguous subunit, as well as the interaction reported by Yamato *et al.*, 2020,[11] by pharmacological assays: hydrogen bonding interaction between the amide group of fluralaner and the carbonyl oxygen of a Glutamine residue (GLN) located in TM1(Figure 2).[11]

In order to characterize the NCA-II binding site of the *Aa*RDL receptor and to better understand the pose and estimated binding affinity of the isoxazolines, docking assays were carried out at this specific binding site using three additional isoxazolines, afoxolaner, lotilaner, and sarolaner (Figure S3 B-D).

Molecular Dynamics Simulations of Canonical Isoxazolines

The binding mode of isoxazolines in RDL receptor needs to be clarified to understand the underlying mechanism of this family mode of action and to develop novel, efficient NCA-II insecticides. Therefore, we carried out MDS based on the pose obtained from molecular docking of fluralaner, afoxolaner, lotilaner, and sarolaner in the *Aa*RDL. Each ligand-receptor complex was embedded in a hydrated lipid bilayer of 512 POPC and simulated for 500 ns at 300 K. We characterized the major ligand-receptor interactions of isoxazolines with the RDL receptor and characterized the dynamics of the binding site.

The overall structural stability of each system was evaluated by calculating the Root Mean Square Deviation (RMSD) of the atomic position for the Transmembrane region (TM) of the protein with and without the bound ligands, as well as for each ligand, throughout all production MDS (Figure S4). To determine the evolution of the system's structural configuration over the simulated time, we calculated the RMSD values of the transmembrane region of the receptor, with and without the bound ligands, and of each compound studied. During the first 100 ns of simulation, an increased RMSD value for all ligands is observed (Figure S4), which is attributed to conformational changes typical of the equilibration of the ligands in the binding site. After this initial time, ligand RMSD values reached a plateau. The RMSD values of the TM of the *Aa*RDL are higher for isoxazolines-bound receptors, reaching values close to 4.5 Å, than for the APO form. This indicates that the binding site undergoes structural changes due to the presence of the compounds for over 500 ns. An exception is observed for fluralaner, which maintains the same RMSD value as the one observed for the apo protein (Figure S4). This could indicate that slight differences exist between the interactions of fluralaner and the rest of the isoxazolines at the pocket.

In order to have an estimate of the spatial stability of the ligands at the binding site, we graphed the spatial displacement of each molecule in the Z axis (Figure S5, right panel), as well as in the xy plane of the membrane (Figure S5, left panel), along the MDS. To determine the relative position of isoxazolines in the Z axis, three residues located at the beginning (MET213, ALA265, LYS274) and three residues at the middle (ILE229, THR252, VAL287) of TM1, TM2, and TM3 of the *Aa*RDL, respectively, were taken as a reference. During the first 150 ns, the compounds moved deeper into the bilayer. After 150 ns, fluralaner and afoxolaner showed a constant depth over time. Meanwhile, lotilaner and sarolaner showed a tendency to move along the Z axis towards the top and middle of the TMs, respectively (Figure S5-right panel). No major displacements were observed for ligands in the XY plane in any of the systems (Figure S5-left panel).

The *Aa*RDL NCA-II site residues found at an average distance less than or equal to 3.5 Å from the isoxazolines, over the 500 ns of simulation, were: GLN219, ILE220, TYR221, PRO223, SER224, ILE227, VAL228, SER231, LEU259, MET260, THR263, ASN264, ALA266, LEU267, SER271, ILE276, LEU280, GLY281, CYS283, PHE284, VAL287, PHE288. After a structural clustering analysis of the isoxazolines over the simulation time, we illustrated the representative hydrophobic interactions of the average structure obtained between the compounds and the rest of the components of the system, using LigPlot software.[42] Also, *Aa*RDL NCA-II site residues found at an average distance less than or equal to 3.5 Å to isoxazolines included: GLN219, ILE220, TYR221, PRO223, SER224, ILE227, VAL228, SER231, LEU259, MET260, THR263, ASN264, ALA266, LEU267, SER271, ILE276, LEU280, GLY281, CYS283, PHE284, VAL287, PHE288. These residues would be involved in hydrophobic interactions with isoxazolines (Figure S6).

Since hydrogen bonds (H-bonds) have been reported to play a key role in the interaction between fluralaner and the receptor,[11] we analyzed their temporal evolution throughout the simulation time (Table 1 and Figure S7). As reported previously,[11] the H-bond interaction with the most significant contribution is the one between the isoxazolines and GLN219, located in the TM1 helix of the receptor (Figure 1). This interaction is maintained for all four isoxazolines analyzed (Table 1). Other residues involved in H-bond interactions are THR257, SER261, SER262, THR263, and ASN264. These interactions are present for fluralaner, afoxolaner, sarolaner, and lotilaner to a lesser extent (Table 1). Fluralaner and afoxolaner made a maximum of 3 H-bonds, with an average of 1.7 during the 500 ns.

Further, we carried out the calculations of the binding free energy (ΔG) between the *AaRDL* receptor and the different isoxazolines using the MMPBSA method and the GMX-MMPBSA software[39,41] and allowed calculations of binding free energy of membrane proteins from trajectories obtained with GROMACS.[29] The calculated energetic contributions for the four ligand-receptor complexes are summarized in Figure 3A, where the compounds exhibit a gradient of affinity for the receptor in the following order: Fluralaner>Sarolaner≳Afoxolaner≳Lotilaner. This ordering reproduces the *in vivo* acaricide efficacy reported for these compounds.[43] For all four systems, the Van der Waals energetic contribution is the one with the highest impact on the binding of isoxazolines to its site (Figure 3B). The ligand-receptor interaction is energetically favorable in vacuum, while disfavorable in solvent ($\Delta E_{MM} < \Delta G_{sol}$), which would indicate that the entry of water molecules into the binding site would disfavor the interaction of the isoxazolines with *Aa*RDL (Figure 3B). This was confirmed by

Table 1: Average H-bonds (AH) and Main residues of the TM of the receptor involved in H-bond interaction with the studied isoxazolines.

	AH	GLN 219	THR 257	THR 258	MET 260	SER 261	SER 262	THR 263	ASN 264	ASP 277	GLY 281
Fluralaner	1.7± 1.0	x	x			x	x	x	x		
Afoxolaner	0.5 ± 0.8	x	x		x	x	x	x	x		
Lotilaner	0.7 ± 1.0	x								x	x
Sarolaner	0.7 ± 0.6	x	x	x	x	x	x	x	x		

the number of H-bond interactions between the isoxazolines and water (Figure S8). Fluralaner, the isoxazoline that had the greatest interaction with the receptor (Figure 3A), is the one that showed the least interaction with water molecules (Figure S8).

Isoxazolines showed structural and spatial stability in their binding site in the *Aa*RDL, without diffusing laterally towards lipids or towards the center of the pore, exploring a range of depths between the protein residues taken as reference. In addition, the receptor residues common in hydrophobic interactions with isoxazolines were identified: ILE218, GLN219, ILE222, PRO223, LEU226, MET260, ASP277, VAL278, GLY281, PHE284, and VAL285, as well as the main *Aa*RDL residues involved in H-bonds with them were also identified: GLN219, THR257, SER261,

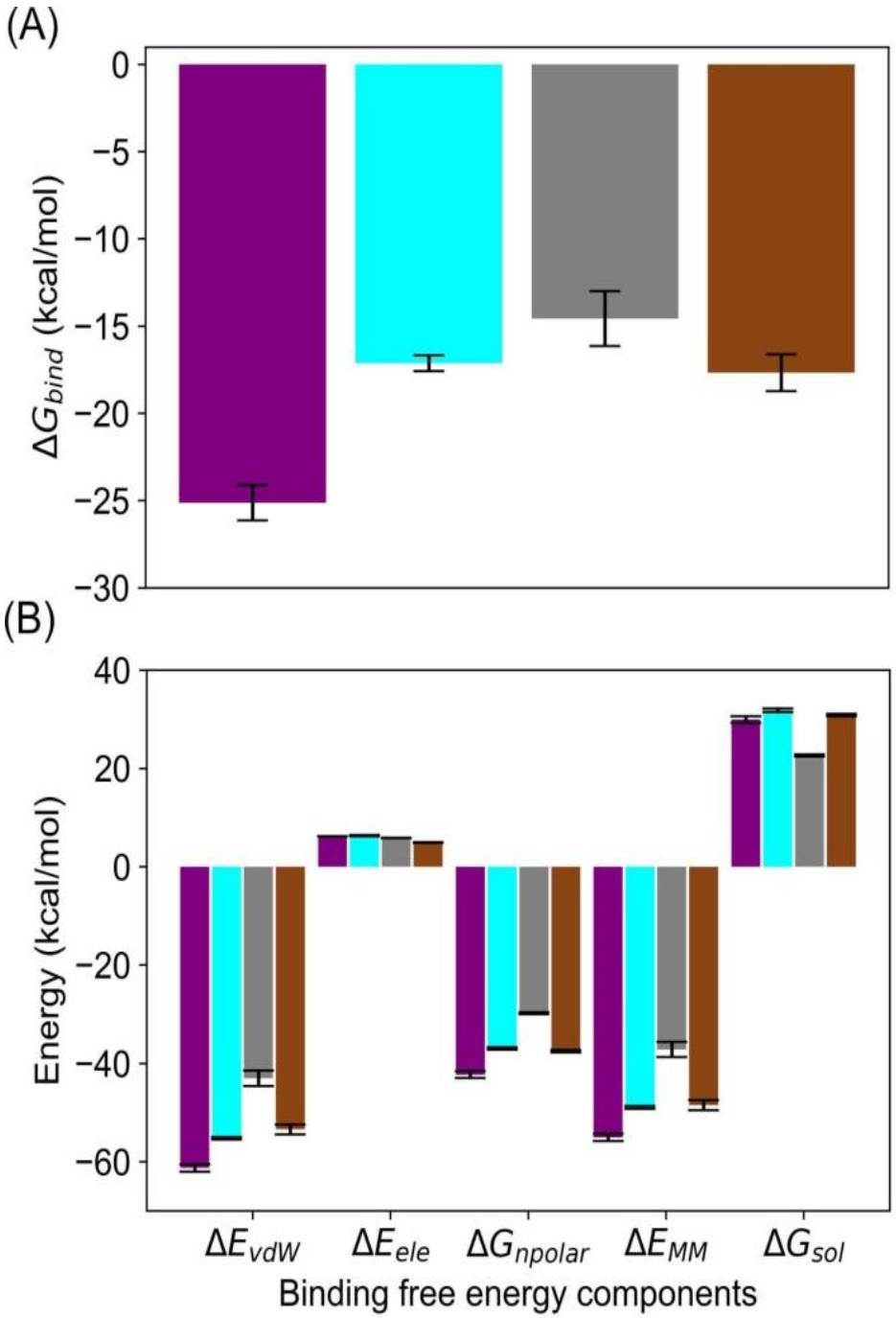

Figure 3: Binding free energy and energetic contribution of each component for every *Aa*RDL-Isoxazoline complex. (A) ΔG_{bind}: Total binding free energy. (B) Decomposition of energetic contributions: ΔE_{vdW}: Van der Waals energies; ΔE_{ele}: electrostatic energies; ΔG_{sol}: solvation energy and ΔE_{npolar}: nonpolar contributions; ΔE_{MM}: molecular mechanical energy in the gas phase. *Aa*RDL-fluralaner (purple), *Aa*RDL-afoxolaner (cyan), *Aa*RDL-lotilaner (grey), and *Aa*RDL-sarolaner (brown). Error bars indicate standard deviation values.

Table 2: Reported quinazoline derivatives with insecticidal activity and compounds obtained in the VS.

Designed code	Scheme of the molecule	Name of the compound in the published work
Q52		Compound 52,[51] Compound 5a,[55] Compound A.[54]
Q53	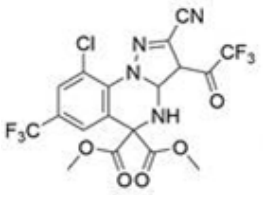	Compound 53,[51] Compound 4a.[54]
Q54	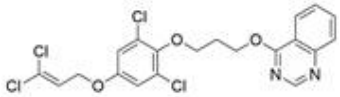	Compound 5451, Compound li.[57]
Q55	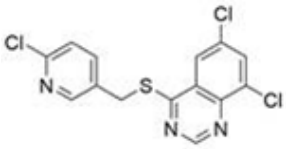	Compound 5551, Compound Vi[52]
Q56	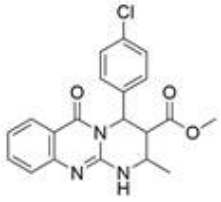	Compound 56,[51] Compound DHPM3.[58]
Q57	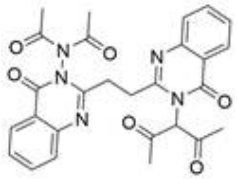	Compound 57,[51] Compound Tetraactyl bis-quinazolinones.[61]
Z952820	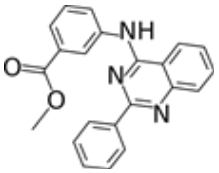	Methyl 3-{[2-(3-methylphenyl) quinazolin-4-yl]amino}benzoate,[62] ZINC952028.[48]

SER262, THR263, and ASN264. Furthermore, it was observed that the energy component with the greatest contribution to the interaction between isoxazolines and the receptor is the Van der Waals energy, and the solvation of the binding site decreases the interaction between isoxazolines and *Aa*RDL.

Virtual Screening

Once we have characterized the main residues responsible for isoxazoline interaction with *Aa*RDL, we then proceed to search for compounds that could potentially target the same binding site. SBVS is a powerful tool that allows users to identify new active drugs that act on a particular target. The validation of a protocol for a VS is a retrospective test that consists of the evaluation of the ability of the docking screening to distinguish between previously known active compounds from inactive ones. Unfortunately, this requires a considerable number of ligands with experimentally determined affinity for the target protein. Isoxazolines represent a new family of GABAergic insecticides, recently developed for which only a few active compounds are known,[2] complicating their validation. Therefore, we used a hybrid protocol, based

on a mixed LB and SBVS (Figure 4A). First, we performed a prospective LBVS,[44] in order to obtain new potential GABAergic compounds. This methodology consists of the design of a pharmacophore,[45] based on the physicochemical properties of the known active ligands, in this case, isoxazolines with reported insecticidal activity. We generated 10 pharmacophore models, and a subsequent validation allowed us to select the best one using the program LigandScout 4.4.[22] For the generation of the pharmacophores, 7 active ligands were used as Training-set ligands (Table S2). These belong to the isoxazoline chemical family, for which experimental affinities with $GABA_AR$ have been determined previously.[2,18] The best generated pharmacophore was selected by measuring its ability to discriminate between active ligands from decoys. We used the other 12 active isoxazolines

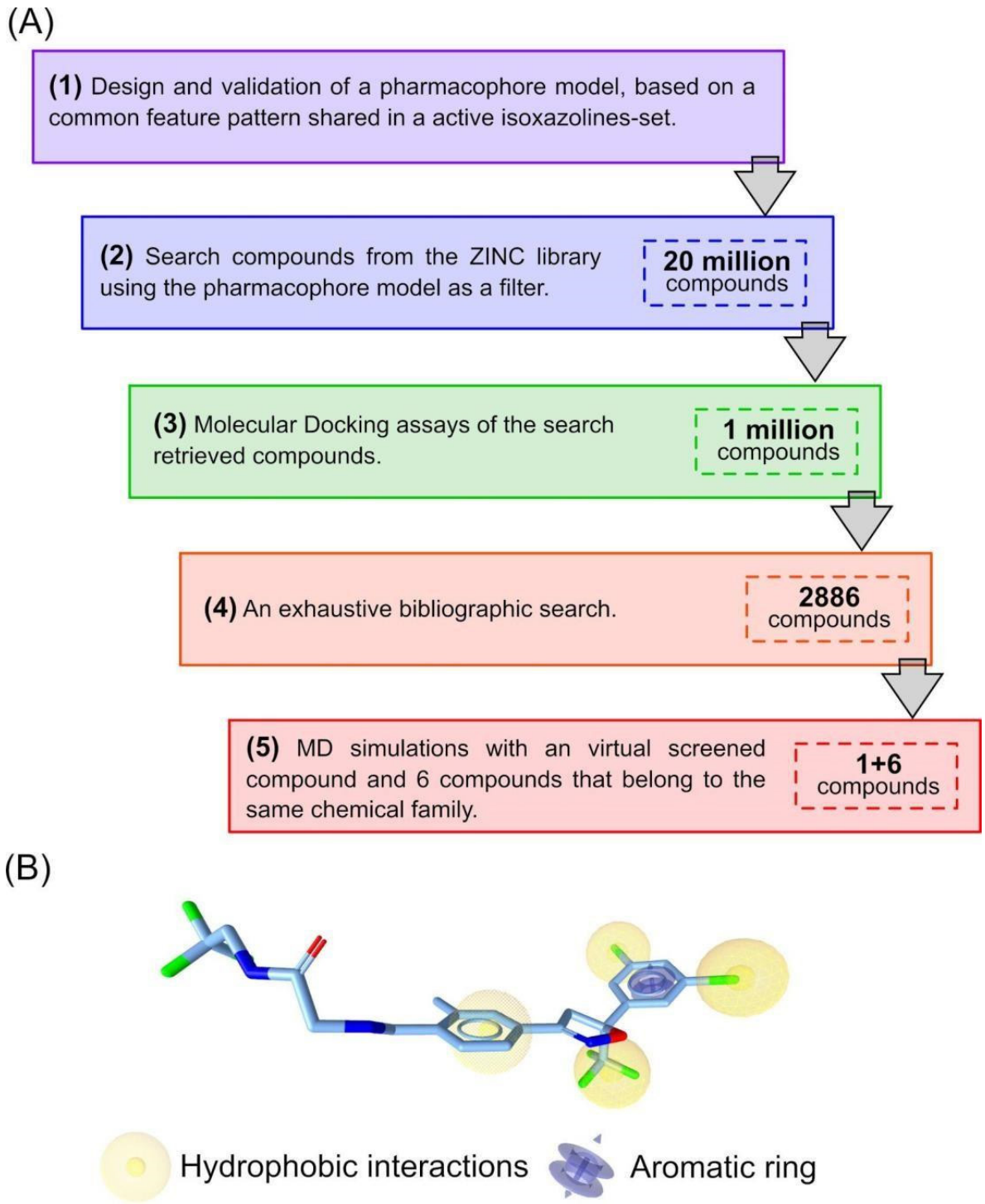

Figure 4: Virtual Screening workflow and pharmacophore model for GABAergic isoxazoline-like insecticides. (A) VS workflow for searching potential GABAergic insecticidal compounds that share the same site of action as isoxazolines. (B) Pharmacophoric characteristics of the best pharmacophore generated in step 1 of the VS workflow.

as Test-set ligands,[2,18] and 650 decoys generated with DUD-E[23] using the test set, as detailed in Table S2. The validation of the model was carried out using LigandScout ROC curve (Receiver Operating characteristic) and AUC (Area Under the ROC curve) analysis with default values (Figure S9).

The selected pharmacophore was used as a filter in a search for purchasable compounds in the ZINC library (https://zinc.docking.org/), that shared similar physicochemical characteristics. In order to expand the search to a wider variety of ligands, we narrowed to five selected characteristics of the pharmacophore (Figure 4B) to recover potential molecules by using the online interface ZINCPharmer.[24] The selection criteria for these pharmacophore features were based on the general structural similarities found between isoxazolines and meta-diamides, such as trifluoromethyl groups, halogen atoms, and aromatic rings. These compounds also act on the ANC-II site of the RDL receptor like isoxazolines.[46,47] This selection retrieved approximately 1 million compounds that shared the desired pharmacophoric characteristics. These molecules were used to carry out prospective SBVS assays, using the AutodockVina program[20] in the NCA-II binding site of the homology model obtained for *Aa*RDL (Figure 1 B-C). These SBVS showed a total of 2886 compounds with high affinity for *Aa*RDL. An exhaustive analysis of the retrieved compounds in the ZINC database[48] was performed in order to obtain information about the biological activity and/or protein target. The compounds ZINC952820 (Z952820), and methyl 3{[2(3-methylphenyl) quinazolin 4-yl]amino}benzoate, although they have no described protein target, have the $GABA_AR$ as a predicted target protein, according to the SEA (Similarity Ensemble Approach) predictor[49] of ChEMBL20.[50] This compound belongs to the quinazoline chemical family, which has several compounds with insecticide and larvicidal activity.[51-53] These quinazolines have no protein target reported that accounts for their insecticidal activity. Even though other binding sites cannot be ruled out for quinazolines, our results gave a hint that these compounds potentially target RDL, and therefore, our next step was to characterize their binding site in detail.

Quinazolines binding site validation and potential selectivity against insects

Quinazoline derivatives have a broad spectrum of biological activities, with a structure formed by the fusion of a benzene with a six-membered ring with 2 nitrogen atoms.[52] The application of the quinazoline scaffold in pesticide discovery has been proposed to be promising in the rational design of novel and safe pesticides. Quinazolines' scaffold have drawn attention because of their versatility to generate derivatives with good herbicidal, antibacterial, and insecticide activity.[54] A quinazoline derivative has shown LC_{50} values against insects such as *Plutella xylostella* superior to those of fipronil, and it has been suggested that it could act as a potent $GABA_AR$ antagonist with binding poses different from those of fipronil. Nevertheless, protein targets have not been described for most insecticidal quinazolines, and the $GABA_AR$ binding site and mechanism of action have yet to be described.[54-57] Given that this family has among its members compounds with reported insecticidal activity[51,55,56] and others with known affinity for $GABA_AR$[57] it is interesting to evaluate the possibility that the insecticide activity is linked to their binding to this RDL as a target, to determine quinazoline's potential action on the RDL, and to characterize the action mechanism. To further validate the quinazolines binding site, we performed Blind Docking assays throughout all the *Aa*RDL TM, using the reported quinazoline derivatives that at present have shown good insecticidal activity[51] as a result, the compound Z952820 was obtained in SBVS (Table 2). The choice to explore this region of the receptor was based on the fact that the NCAs have their binding sites in this area.[58] All quinazolines analyzed were bound at the interface between two adjacent subunits, between TM1 of one subunit and TM3 of the adjacent subunit (Figure S10), as isoxazolines do. Therefore, insecticidal quinazolines could share the preference for the same binding site at *Aa*RDL as isoxazolines.

Furthermore, with the purpose of exploring the potential selectivity of quinazolines, we performed blind docking assays of both isoxazolines (Figure 1A) and quinazolines (Table 2) using mammal $GABA_AR$[26] assessing the potential toxic effects on vertebrates of all the molecules under study. The results demonstrated that isoxazolines (fluralaner, afoxolaner, lotilaner, and sarolaner) are bound to the external surface of the mammal $GABA_AR$ (Figure S11), not reaching the interfacial site between

Table 3: Residues of the TM of the RDL receptor that interact with the analyzed compounds.

	AH	GLN 219	THR 255	THR 257	THR 258	SER 261	SER 262	ASN 264	ASP 277	GLY 281	THR 282	ASN 331
Z952820	0.2 ± 0.4	x	x	x		x		x				
Q54	0.4 ± 0.6	x			x	x	x	x				
Q55	0.1 ± 0.2			x				x				
Q56	0.2 ± 0.4								x	x	x	
Q57	0.2 ± 0.4											x

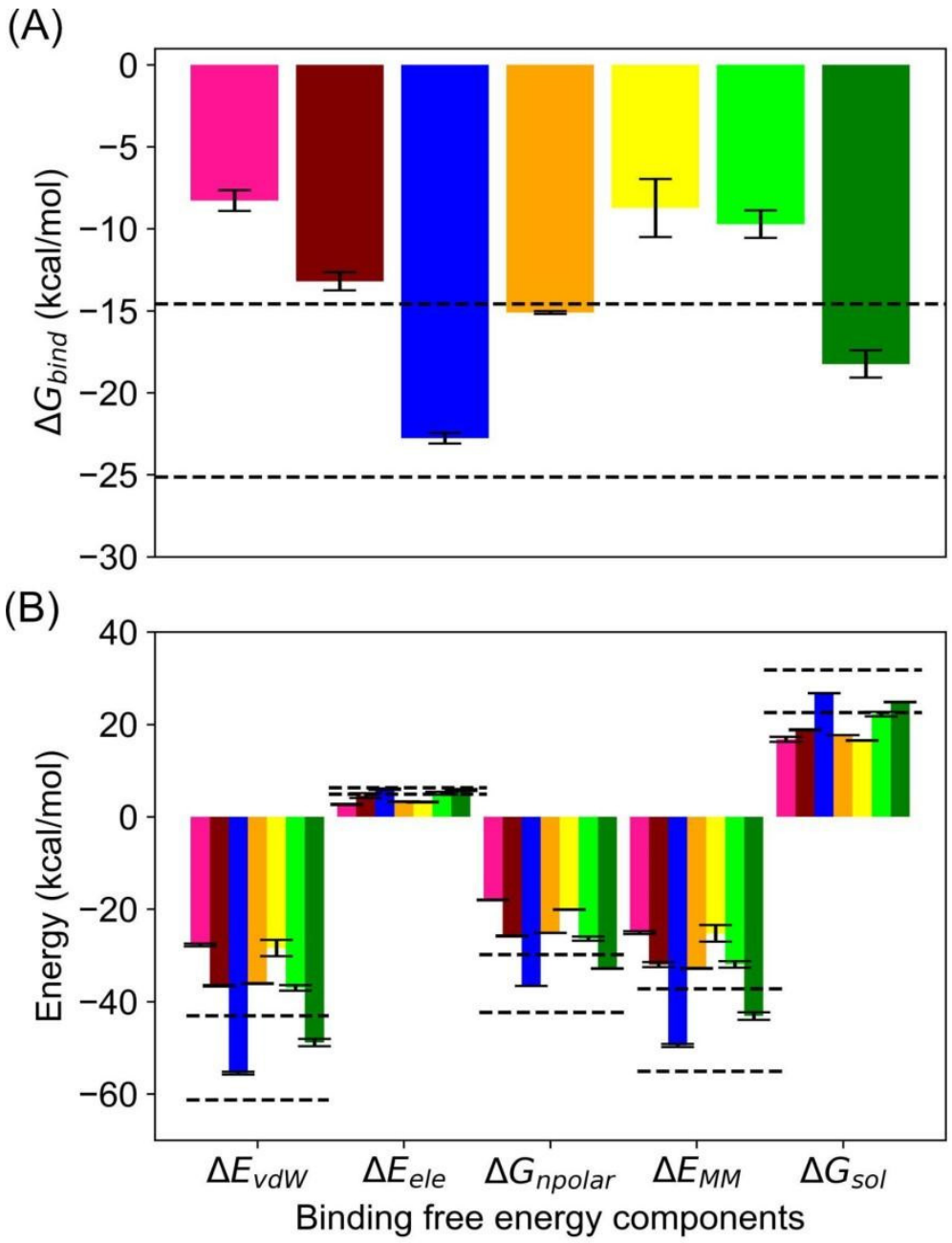

Figure 5: (A) Binding free energy and (B) energetic contribution of each component for every *Aa*RDL-Quinazoline complex. Q52 (pink), Q53 (maroon), Q54 (blue), Q55 (orange), Q56 (yellow), Q57 (lime), Z952820 (green). Error bars indicate standard deviation values. ΔG_{bind}: binding free energy. Components: ΔE_{vdW}: Van der Waals energies; ΔE_{ele}: electrostatic energies; ΔG_{sol}: solvation energy and ΔE_{npolar}: nonpolar contributions; ΔE_{MM}: molecular mechanical energy in the gas phase. The maximum and minimum value of ΔG_{bind} and each component obtained for isoxazolines are represented in dotted lines.

TM1 and TM3, where they bind in RDL. Similarly, the preferential location of most of the quinazolines was also on the external face of the receptor in the area of the TM (Figure S12). This behavior, similar to that observed in isoxazolines[1,10,59] would indicate that this novel family of compounds could also present a selective toxicity for insects over mammals, since it presents the same pattern.

Molecular Dynamics Simulations of Quinazolines

We carried out 500 ns MDS using the complex obtained from molecular docking in the *Aa*RDL receptor model of quinazolines with reported insecticide activity[51] including the compound obtained in the VS, Z952820, that belongs to this family (Table 2). We characterized the quinazoline-*Aa*RDL interactions and compared the results with those obtained for isoxazolines in order to confirm the results from docking assays that these compounds could share the target pocket.

RMSD values of the systems with Q52-57 at the allosteric NCA-II site were obtained to determine their stability at the pocket (Figure S13). RMSD values of the TM of RDL are higher for the holo form of the receptor than for the apo form. This indicates that the binding site is molding to the compounds. Q55 and Q57 showed the highest RMSD values, while Q53 and Q54 were the most stable quinazolines. RMSD values of Z952820 at the blocking site show good stability. In contrast, the RMSD values of the TM of the receptor with and without this ligand bound reflect a conformational change in this area throughout the 500 ns of simulation. In all cases, the RMSD values do not exceed 4.5 Å. For the purpose of analyzing the spatial stability of quinazolines at the binding site of the isoxazolines, we calculated the temporal evolution of the position of each molecule in the Z axis and the XY plane, up to 500 ns. Three residues located at the beginning (MET213, ALA265, LYS274) and three residues at the middle (ILE229, THR252, VAL287) of TM1, TM2, and TM3 of the *Aa*RDL, respectively, were taken as a reference for the relative position of the quinazolines in the Z axis vs Time graphs. The quinazolines Q54, Q56, and Q57 demonstrated lateral movement in the XY plane of the membrane, at the interface between the two adjacent subunits, without diffusing into the lipids or towards the center of the pore over the course of 500 ns. The displacement was similar to the one observed for isoxazolines, except that Quinazoline Q54 exhibited the greatest lateral displacement, moving from one interface of the homopentamer to another, moving across the TM of *Aa*RDL. Most Quinazolines are situated closer to the reference residues located at the middle of the TM1, TM2, and TM3 of the *Aa*RDL compared to Z952820 and isoxazolines. On the other hand, Z952820 is located near the reference residues located at the beginning of the TM1, TM2, and TM3 of the *Aa*RDL. The spatial displacement shown by quinazolines is within the scale observed for 2 isoxazolines.

The main interactions reported for canonical isoxazolines in *Aa*RDL binding site are H-bonds with residues GLN219, THR257, SER261, SER262, THR263, and ASN264. By calculating the number of H-bond interactions as a function of time for each quinazoline, it was observed that five out of these six residues are forming H-bonds with Q54 and Z952820. Q55 interacts with two of these residues, and Q56 and Q57 interact with other residues of the receptor, other than the main ones. Q52 and Q53 do not establish this type of interaction with the *Aa*RDL (Table 3).

We carried out ΔG calculations of *Aa*RDL receptor interaction with the different quinazolines using the MMPBSA[39] (Figure 5). Q54, Q55, and Z952820 presented affinities (Figure 5A) within the ones found for canonical isoxazolines (see Figure 3A), Q54 presenting the highest affinity. Q54 and Z952820, which can form H-bonds with GLN219, are the ones with the greatest affinity. Therefore, H-bonds with this residue could be considered as highly relevant for the pocket activity, and considered when designing new compounds. This is consistent with the fact that this interaction is the only H-bond conserved in all the isoxazolines analyzed (see Table 1). Finally, the largest contribution to the interaction of quinazolines with *Aa*RDL is Van der Waals interactions (Figure 5B), as it was observed for isoxazolines (see Figure 3B). Similar to the observed with isoxazolines-*Aa*RDL, the quinazolines-*Aa*RDL interactions are energetically favorable in vacuum, while unfavorable in solvent ($\Delta E_{MM} < \Delta G_{sol}$). The ones that had the highest interaction with the receptor showed lower H-bonds with water (Q54, Q55, and Z952820) and vice versa, where Q52, Q53, Q56, and Q57 were the ones that interacted the most with the solution (Figure 5A).

The *Aa*RDL residues found at an average distance less than or equal to 3.5 Å from the quinazolines, during the simulated time, were ILE218, GLN219, PRO223, SER224, ILE227, ILE230, THR255, LEU259, SER262, SER275, TYR279, LEU280, THR282, CYS283, MET286, VAL287, and SER290. Some of which could be involved in hydrophobic interactions with these compounds.

Most of the quinazolines exhibited structural and spatial stability in the isoxazoline binding site in the *Aa*RDL, without diffusing laterally towards lipids or the center of the pore, and explored a range of depths within the site, similar to isoxazolines. In addition, the receptor residues common in hydrophobic interactions with quinazolines and isoxazolines were identified, along with the common *Aa*RDL residues of the H-bond interaction with both quinazolines and isoxazolines. Furthermore, it was observed that the energy component with the greatest contribution to the interaction between quinazolines and the receptor is the Van der Waals energy, and the solvation of the binding site decreases the interaction between quinazolines and *Aa*RDL, such as isoxazolines. The comparative analysis of the energies obtained for each component of the free energy of binding of both isoxazolines and quinazolines reinforces the idea that the compounds studied share the same binding site in the *Aa*RDL.

Quinazolines share the same interactions that are responsible for isoxazolines' selectivity

It is essential that new potential insecticides are developed to exhibit high selectivity towards insects, with minimal toxicity to mammals. Differences in the primary structure at the NCA-II site of the RDL subunit and of each subunit of the mammalian $GABA_AR$ have been proposed to contribute to the greater sensitivity to isoxazolines of insects compared to that of mammals.[60] A multiple alignment was performed on the primary sequence of the TM of the RDL subunit of the *Aa*RDL model, and the same region of the α1, β2, and γ2 subunits of the mammalian $GABA_AR$. There are 43 residues in the TM of *Aa*RDL that are not present in the α1, β2, and γ2 subunits of the mammalian $GABA_AR$. Particularly, differences were observed in residues that in the literature are indicated as key for the interaction with isoxazolines. GLY281 of the α M3 helix of *Aa*RDL corresponds to a MET residue in the β2 subunit of the mammalian $GABA_AR$. GLY

to MET mutation at this position has been reported to abolish the inhibitory activity of desmethyl-broflanilide, a negative allosteric modulator that shares the isoxazoline binding site.[21] GLY281 residue has contacts through hydrophobic interactions with all 4 canonical isoxazolines analyzed (Figure 2). Furthermore, MET260 of the α M2 helix of *Aa*RDL residue also has large hydrophobic contacts with isoxazolines (Figure 2). This position is occupied by SER, ASN, and SER residues in α1, β2, and γ2 subunits of the mammalian $GABA_AR$, respectively. This creates an NCA-II action site in mammals that is relatively insensitive to isoxazolines. This set of differences identified in the amino acid sequence of *Aa*RDL compared to mammalian $GABA_AR$ subunits, particularly at the NCA-II site, may contribute to the selective toxicity noted in isoxazolines and potentially in compounds derived from the SV.

CONCLUSION

The discovery of new scaffolds for GABAergic pesticides is a huge and required challenge, because of the development of resistance to conventional insecticides acting as $GABA_AR$ antagonists and the need to develop safer insecticides. We aim to develop *in silico* protocols that allow us to speed up the discovery of new noncompetitive antagonist inhibitors of $GABA_AR$ that present higher selectivity for insect pests, showing minimal effects on mammals. A hybrid ligand- and structure-based prospective database screening and MDS validation proved to be a promising tool not only for the search for new potential insecticides, but also for the search for the protein target of already described insecticides. Taken together, our results provide *in silico* evidence for both isoxazolines and quinazolines acting on the same insect $GABA_AR$ binding site.

ACKNOWLEDGEMENT

M.S.G. is a doctoral fellow from CONICET. M.E.S-B, D.A.G., and V.M. are Scientific Research Career members of CONICET. This work was supported by CONICET and SECyT-UNC. This work used computational resources from CCAD-Universidad Nacional de Córdoba (http://ccad.unc.edu.ar/).

ABBREVIATIONS

GABA: γ-aminobutyric acid; **$GABA_AR$:** $GABA_A$ receptor; **NCA:** Noncompetitive antagonist; **RDL:** Insect $GABA_AR$ resistent to dieldrin; **TM:** Transmembrane región; **TSI:** Transmembrane subunit interface; **VS:** Virtual screening; **SB:** Structure-based; **QSAR:** Quantitative structure-activity relationship; **SAR:** Structure-activity relationship; **SAR:** Retrospective virtual screening; **LB:** Ligand-based; **AaRDL:** *Aedes aegypti* RDL receptor; **GLUC:** Glutamate-gated chloride channel; **MDS:** Molecular Dynamics Simulations; **POPC:** Palmitoyl-oleoyl phosphatidylcholine; **RESP:** Restrained Electrostatic Potential; **ACPYPE:** AnteChamber Python Parser; **MMPBSA:** Molecular Mechanics/Poisson–Boltzmann Surface Area; **SASA:** Solvent Accessible Surface Area; **ROC:** Receiver Operating characteristic; **AUC:** Area Under the Curve; **SEA:** Similarity Ensemble Approach.

CONFLICT OF INTEREST

The authors declare that there is no conflict of interest.

FUNDING

This work was supported by grants from SECyT-UNC (Consolidar 2020 and 2023) and CONICET-Argentina (PIP-2021). KNV thanks the Deanship of Scientific Research, Vice Presidency for Graduate Studies and Scientific Research, King Faisal University, Al-Ahsa, Saudi Arabia [Grant No. KFU254236], and Durban University of Technology, as well as the National Research Foundation of South Africa (Grant number 129330), for their support and encouragement.

DATA AND SOFTWARE AVAILABILITY STATEMENT

All molecular structures and their topologies are available as Supplementary Material, allowing reproducibility of all MDS and Docking Assays results (see All_Systems_coordinates_in_PDB.pdf and All_ligands_Topologies in itp format.pdf).

SUMMARY

We developed a computational *in silico* protocol aimed at accelerating the discovery of novel GABAergic insecticides with enhanced selectivity for insect pests and minimal impact on mammals. Our approach integrates hybrid ligand- and structure-based prospective database screening with Molecular Dynamics Simulation (MDS) validation, targeting compounds that interact with the isoxazoline binding site. Through this process, we gained deeper insights into the binding mechanisms and modes of action of isoxazolines on RDL receptors. Notably, our screening protocol also identified a distinct family of compounds-quinazolines-with previously reported insecticidal and larvicidal activity. These compounds were found to recognize the NCA-II binding site of the RDL receptor, a target that had not been previously associated with any known protein. This protocol demonstrates strong potential not only for identifying new insecticidal candidates but also for uncovering the molecular targets of existing insecticides.

REFERENCES

1. Ozoe Y, Asahi M, Ozoe F, Nakahira K, Mita T. The antiparasitic isoxazoline A1443 is a potent blocker of insect ligand-gated chloride channels. Biochem Biophys Res Commun. 2010;391(1):744-9. doi: 10.1016/j.bbrc.2009.11.131, PMID 19944072.
2. Gonçalves IL, Machado Das Neves G, Porto Kagami L, Eifler-Lima VL, Merlo AA. Discovery, development, chemical diversity and design of isoxazoline-based insecticides. Bioorg Med Chem. 2021;30:115934. doi: 10.1016/j.bmc.2020.115934, PMID 33360575.
3. Rodriguez MA, Felsztyna I, García DA, Sánchez-Borzone ME, Miguel V. Interaction of fluralaner with binary model membranes. Potential implications in the selectivity for invertebrates/vertebrates. J Mol Liq. 2024;403:124891. doi: 10.1016/j.molliq.2024.124891.

4. Huang QT, Sheng CW, Jiang J, Jia ZQ, Han ZJ, Zhao CQ, *et al.* Functional integrity of honeybee (Apis mellifera L.) resistant to dieldrin Γ-aminobutyric acid receptor channels conjugated with three fluorescent proteins. Insect Mol Biol. 2019;28(3):313-20. doi: 10.1111/imb.12552, PMID 30421825.
5. Zheng N, Cheng J, Zhang W, Li W, Shao X, Xu Z, *et al.* Binding difference of fipronil with GABAA Rs in fruitfly and Zebrafish: insights from homology modeling, docking, and Molecular Dynamics simulation studies. J Agric Food Chem. 2014;62(44):10646-53. doi: 10.1021/jf503851z, PMID 25302733.
6. Zhou X, Hohman AE, Hsu WH. Current review of isoxazoline ectoparasiticides used in veterinary medicine. J Vet Pharmacol Ther. 2022;45(1):1-15. doi: 10.1111/jvp.12959, PMID 33733534.
7. Simon J, Wakimoto H, Fujita N, Lalande M, Barnard EA. Analysis of the set of GABAA receptor genes in the human genome. J Biol Chem. 2004;279(40):41422-35. doi: 10.1074/jbc.M401354200, PMID 15258161.
8. Buckingham SD, Biggin PC, Sattelle BM, Brown LA, Sattelle DB. Insect GABA receptors: splicing, editing, and targeting by antiparasitics and insecticides. Mol Pharmacol. 2005;68(4):942-51. doi: 10.1124/mol.105.015313, PMID 16027231.
9. Bormann J. The 'ABC' of GABA receptors. Trends Pharmacol Sci. 2000;21(1):16-9. doi: 10.1016/S0165-6147(99)01413-3, PMID 10637650.
10. Casida JE, Durkin KA, GABA N. Novel GABA Receptor pesticide targets. Pestic Biochem Physiol. 2015;121:22-30. doi: 10.1016/j.pestbp.2014.11.006, PMID 26047108.
11. Yamato K, Nakata Y, Takashima M, Ozoe F, Asahi M, Kobayashi M, *et al.* Effects of intersubunit amino acid substitutions on GABA receptor sensitivity to the ectoparasiticide fluralaner. Pestic Biochem Physiol. 2020;163:123-9. doi: 10.1016/j.pestbp.2019.11.001, PMID 31973848.
12. Sheng CW, Huang QT, Liu GY, Ren XX, Jiang J, Jia ZQ, *et al.* Neurotoxicity and mode of action of fluralaner on honeybee Apis mellifera L. Pest Manag Sci. 2019;75(11):2901-9. doi: 10.1002/ps.5483, PMID 31081291.
13. Felsztyna I, Villarreal MA, García DA, Miguel V, Insect RD. Insect RDL Receptor models for virtual screening: impact of the template conformational state in pentameric ligand-gated ion channels. ACS Omega. 2022;7(2):1988-2001. doi: 10.1021/acsomega.1c05465, PMID 35071887.
14. Salmaso V, Moro S. Bridging molecular docking to Molecular Dynamics in exploring ligand-protein recognition process: an overview. Front Pharmacol. 2018;9:923. doi: 10.3389/fphar.2018.00923, PMID 30186166.
15. Isarankura-Na-Ayudhya C, Naenna T, Nantasenamat C, Prachayasittikul V. A practical overview of quantitative structure-activity relationship. Excli J. 2009; 8. doi: 10.17877/DE290R-690.
16. Glaab E. Building a virtual ligand screening pipeline using free software: A survey. Brief Bioinform. 2016;17(2):352-66. doi: 10.1093/bib/bbv037, PMID 26094053.
17. Jaiteh M, Rodríguez-Espigares I, Selent J, Carlsson J. Performance of virtual screening against GPCR homology models: impact of template selection and treatment of Binding Site plasticity. PLOS Comput Biol. 2020;16(3):e1007680. doi: 10.1371/journal.pcbi.1007680, PMID 32168319.
18. Zhao C, Casida JE. Insect γ-aminobutyric acid receptors and isoxazoline insecticides: toxicological profiles relative to the binding sites of [^{3}H]fluralaner, [^{3}H]-4′-ethynyl-4-n-propylbicycloorthobenzoate, and [^{3}H]avermectin [3 H]Fluralaner, [3 H]-4′-Ethynyl-4- n -Propylbicycloorthobenzoate, and [3 H]Avermectin. J Agric Food Chem. 2014;62(5):1019-24. doi: 10.1021/jf4050809, PMID 24404981.
19. Webb B, Sali A. Comparative protein structure modeling using MODELLER. Curr Protoc Bioinformatics. 2016;54(1):5.6.1-5.6.37. doi: 10.1002/cpbi.3, PMID 27322406.
20. Trott O, Olson AJ, Vina AD. AutoDock Vina: Improving the speed and accuracy of docking with a new scoring function, efficient optimization, and multithreading. J Comput Chem. 2010;31(2):455-61. doi: 10.1002/jcc.21334, PMID 19499576.
21. Gao Y, Zhang Y, Wu F, Pei J, Luo X, Ju X, *et al.* Exploring the interaction mechanism of desmethyl-broflanilide in insect GABA receptors and screening potential antagonists by in silico simulations. J Agric Food Chem. 2020;68(50):14768-80. doi: 10.1021/acs.jafc.0c05728, PMID 33274636.
22. Wolber G, Langer T. LigandScout: 3-D pharmacophores derived from protein-bound ligands and their use as virtual screening filters. J Chem Inf Model. 2005;45(1):160-9. doi: 10.1021/ci049885e, PMID 15667141.
23. Mysinger MM, Carchia M, Irwin JJ, Shoichet BK. Directory of useful decoys, enhanced (DUD-E): better ligands and decoys for better benchmarking. J Med Chem. 2012;55(14):6582-94. doi: 10.1021/jm300687e, PMID 22716043.
24. Koes DR, Camacho CJ. ZINCPharmer: pharmacophore search of the ZINC database. Nucleic Acids Res. 2012; 40(Web Server issue):W409-14. doi: 10.1093/nar/gks378, PMID 22553363.
25. Goetz T, Arslan A, Wisden W, Wulff P. GABAA receptors: structure and function in the basal ganglia. Prog Brain Res. 2007;160:21-41. doi: 10.1016/S0079-6123(06)60003-4, PMID 17499107.
26. Kim JJ, Gharpure A, Teng J, Zhuang Y, Howard RJ, Zhu S, *et al.* Shared structural mechanisms of general anaesthetics and benzodiazepines. Nature. 2020;585(7824):303-8. doi: 10.1038/s41586-020-2654-5, PMID 32879488.
27. Agarwal R, Smith JC. Speed vs accuracy: effect on ligand pose accuracy of varying box size and exhaustiveness in AutoDock Vina. Mol Inform. 2023;42(2):e2200188. doi: 10.1002/minf.202200188, PMID 36262028.
28. Schmidt TH, Kandt C. LAMBADA and InflateGRO2: efficient membrane alignment and insertion of membrane proteins for Molecular Dynamics simulations. J Chem Inf Model. 2012;52(10):2657-69. doi: 10.1021/ci3000453, PMID 22989154.
29. Abraham MJ, Murtola T, Schulz R, Páll S, Smith JC, Hess B, *et al.* GROMACS: high performance Molecular Simulations through multi-level parallelism from laptops to supercomputers. SoftwareX. 2015; 1-2:19-25. doi: 10.1016/j.softx.2015.06.001.
30. Hornak V, Abel R, Okur A, Strockbine B, Roitberg A, Simmerling C. Comparison of multiple Amber force fields and development of improved protein backbone parameters. Proteins. 2006;65(3):712-25. doi: 10.1002/prot.21123, PMID 16981200.
31. Jämbeck JP, Lyubartsev AP. Derivation and systematic validation of a refined all-atom force field for phosphatidylcholine lipids. J Phys Chem B. 2012;116(10):3164-79. doi: 10.1021/jp212503e, PMID 22352995.
32. Jorgensen WL, Chandrasekhar J, Madura JD, Impey RW, Klein ML. Comparison of simple potential functions for simulating liquid water. J Chem Phys. 1983;79(2):926-35. doi: 10.1063/1.445869.
33. Nosé S. A unified formulation of the constant temperature Molecular Dynamics methods. J Chem Phys. 1984;81(1):511-9. doi: 10.1063/1.447334.
34. Hoover WG. Canonical dynamics: equilibrium phase-space distributions. Phys Rev A Gen Phys. 1985;31(3):1695-7. doi: 10.1103/PhysRevA.31.1695, PMID 9895674.
35. Parrinello M, Rahman A. Polymorphic transitions in single crystals: A new Molecular Dynamics method. J Appl Phys. 1981;52(12):7182-90. doi: 10.1063/1.328693.
36. Frisch MJ, Trucks GW, Schlegel HB, Scuseria GE, Robb MA, Cheeseman JR, *et al.* Gaussian. Vol. 09 & Gaussian 03; 2009.
37. Wang J, Wolf RM, Caldwell JW, Kollman PA, Case DA. Development and testing of a General Amber force field. J Comput Chem. 2004;25(9):1157-74. doi: 10.1002/jcc.20035, PMID 15116359.
38. Sousa Da Silva AW, Vranken WF, ACPYPE, AnteChamber P. ACPYPE – AnteChamber PYthon parser interfacE. BMC Res Notes. 2012;5(1):367. doi: 10.1186/1756-0500-5-367, PMID 22824207.
39. Valdés-Tresanco MS, Valdés-Tresanco ME, Valiente PA, Moreno E. gmx_MMPBSA: A new tool to perform end-state free energy calculations with GROMACS. J Chem Theor Comput. 2021;17(10):6281-91. doi: 10.1021/acs.jctc.1c00645, PMID 34586825.
40. Case DA, Aktulga HM, Belfon K, Ben-Shalom IY, Berryman JT, Brozell SR, *et al.* 2023.
41. Miller BR, McGee TD, Swails JM, Homeyer N, Gohlke H, Roitberg AE. MMPBSA.py: an efficient program for end-state free energy calculations. MMPBSA.py \h hlke. J Chem Theor Comput. 2012;8(9):3314-21. doi: 10.1021/ct300418h, PMID 26605738.
42. Laskowski RA, Swindells MB. LigPlot+: multiple ligand-protein interaction diagrams for drug discovery. J Chem Inf Model. 2011;51(10):2778-86. doi: 10.1021/ci200227u, PMID 21919503.
43. Burgio F, Meyer L, Armstrong R. A comparative laboratory trial evaluating the immediate efficacy of fluralaner, afoxolaner, Sarolaner and Imidacloprid + permethrin against adult Rhipicephalus Sanguineus (sensu lato) ticks attached to dogs. Parasit Vectors. 2016;9(1):626. doi: 10.1186/s13071-016-1900-z, PMID 27912787.
44. Ripphausen P, Nisius B, Peltason L, Bajorath J. Quo vadis, virtual screening? A comprehensive survey of prospective applications. J Med Chem. 2010;53(24):8461-7. doi: 10.1021/jm101020z, PMID 20929257.
45. Geppert H, Vogt M, Bajorath J. Current trends in ligand-based virtual screening: molecular representations, data mining methods, new application areas, and performance evaluation. J Chem Inf Model. 2010;50(2):205-16. doi: 10.1021/ci900419k, PMID 20088575.
46. Nakao T, Banba S. Minireview: mode of action of meta-diamide insecticides. Pestic Biochem Physiol. 2015;121:39-46. doi: 10.1016/j.pestbp.2014.09.010, PMID 26047110.
47. Wu J, Dang S, Zhang Y, Zhou S. Novel meta-diamide compounds containing sulfide derivatives were designed and synthesized as potential pesticides. Molecules. 2024;29(6):1337. doi: 10.3390/molecules29061337, PMID 38542973.
48. Sterling T, Irwin JJ. Zinc 15 – ligand discovery for everyone. J Chem Inf Model. 2015;55(11):2324-37. doi: 10.1021/acs.jcim.5b00559, PMID 26479676.
49. Keiser MJ, Roth BL, Armbruster BN, Ernsberger P, Irwin JJ, Shoichet BK. Relating protein pharmacology by ligand chemistry. Nat Biotechnol. 2007;25(2):197-206. doi: 10.1038/nbt1284, PMID 17287757.
50. Davies M, Nowotka M, Papadatos G, Dedman N, Gaulton A, Atkinson F, *et al.* ChEMBL Web services: streamlining access to drug discovery data and utilities. Nucleic Acids Res. 2015; 43(W1):W612-20. doi: 10.1093/nar/gkv352, PMID 25883136.
51. Chen J, Wang Y, Luo X, Chen Y. Recent research progress and outlook in agricultural chemical discovery based on quinazoline scaffold. Pestic Biochem Physiol. 2022;184:105122. doi: 10.1016/j.pestbp.2022.105122, PMID 35715060.
52. Wu J, Bai S, Yue M, Luo LJ, Shi QC, Ma J, *et al.* Synthesis and insecticidal activity of 6,8-dichloro-quinazoline derivatives containing a sulfide substructure. Chem Pap. 2014;68(7). doi: 10.2478/s11696-014-0540-z.
53. Quinoline, quinazoline y Cinoline derivatives. Available from: https://patents.google.com/patent/GT198900008A/es.
54. Yang S, Lai Q, Lai F, Jiang X, Zhao C, Xu H. Design, synthesis, and insecticidal activities of novel 5-substituted 4, 5-dihydropyrazolo [1,5- a]quinazoline derivatives. Pest Manag Sci. 2021;77(2):1013-22. doi: 10.1002/ps.6113, PMID 33002298.
55. Jiang X, Yang S, Yan Y, Lin F, Zhang L, Zhao W, *et al.* Design, synthesis, and insecticidal activity of 5,5-disubstituted 4,5-dihydropyrazolo[1,5- a]quinazolines as novel antagonists of GABA receptors. J Agric Food Chem. 2020;68(50):15005-14. doi: 10.1021/acs.jafc.0c02462, PMID 33269911.

56. Li J, Wang ZY, Wu QY, Yang GF. Design, synthesis and insecticidal activity of novel 1,1-dichloropropene derivatives. Pest Manag Sci. 2015;71(5):694-700. doi: 10.1002/ps.3827, PMID 24817508.
57. Venugopala KN, Nayak SK, Gleiser RM, Sanchez-Borzone ME, Garcia DA, Odhav B. Synthesis, polymorphism, and insecticidal activity of methyl 4-(4-chlorophenyl)-8-iodo-2-methyl-6-oxo-1,6-dihydro-4 H-pyrimido[2,1-b]quinazoline-3-carboxylate against anopheles arabiensis mosquito. Chem Biol Drug Des. 2016;88(1):88-96. doi: 10.1111/cbdd.12736, PMID 26841246.
58. Weber T, Selzer PM. Isoxazolines: A novel chemotype highly effective on ectoparasites. ChemMedChem. 2016;11(3):270-6. doi: 10.1002/cmdc.201500516, PMID 26733048.
59. Cassayre J, Smejkal T, Blythe J, Hoegger P, Renold P, Pitterna T, *et al.* The discovery of Isocycloseram: A novel isoxazoline insecticide. In: Recent highlights in the discovery and optimization of crop protection products. Elsevier; 2021. p. 165-212. doi: 10.1016/B978-0-12-821035-2.00008-5.
60. Zhang Y, Huang Q, Sheng C, Liu G, Zhang K, Jia Z, *et al.* G3'MTMD3 in the insect GABA receptor subunit, RDL, confers resistance to broflanilide and fluralaner. PLOS Genet. 2023;19(6):e1010814. doi: 10.1371/journal.pgen.1010814, PMID 37384781.
61. Elshahawi MM, EL-Ziaty AK, Morsy JM, Aly AF. Synthesis and insecticidal efficacy of novel bis quinazolinone derivatives. J Heterocycl Chem. 2016;53(5):1443-8. doi: 10.1002/jhet.2445.
62. MolPort. Methyl 3-{[2-(3-Methylphenyl)Quinazolin-4-Yl]Amino}benzoate. MolPort.; n.d. [cited Oct 1, 2025] Available from: Https://Www.Molport.Com/Shop/Compound/Molport-000-664-688.

Cite this article: Gastaldi MS, Sánchez-Borzone ME, Deb PK, Kar S, Venugopala KN, García DA, Miguel V. Molecular Dynamics Characterization of the NCA-II Binding Site in Insect GABAA Receptors and Its Application to Ligand Screening. Indian J of Pharmaceutical Education and Research. 2026;60(2s):s507-s521.